ISSN 1023-1935, Russian Journal of Electrochemistry, 2017, Vol. 53, No. 10, pp. 1232–1238. © Pleiades Publishing, Ltd., 2017.
Original Russian Text © A.S. Berezin, R.R. Nazmutdinov, 2017, published in Elektrokhimiya, 2017, Vol. 53, No. 10, pp. 1390–1397.

Monte Carlo Simulations of Heterogeneous Electron Transfer: New Challenges[1, 2]

A. S. Berezin and R. R. Nazmutdinov*

Kazan National Research Technological University, Kazan, 420015 Russia

**e-mail: nazmutdi@mail.ru*

Received February 14, 2017; in final form, April 4, 2017

Abstract—We report results of MC simulations of electron transfer across a metal electrode/electrolyte solution interface. The model presumes the Landau–Zener theory and a random walk on a two-dimensional lattice formed by crossing parabolic reaction free energy surfaces along the solvent coordinate. Emphasis is put on investigating the activationless discharge regime; the bridge-assisted electron transfer is also partially addressed. We have calculated effective electronic transmission coefficient as a function of the electrode overpotential and temperature in a wide range of orbital overlap. The dependence of the transmission coefficient on the electronic density of states is analyzed as well.

Keywords: electron transfer, Monte Carlo simulations, electronic transmission coefficient, activationless discharge, bridge-assisted electron transfer

DOI: 10.1134/S1023193517100032

1. INTRODUCTION

The elementary act of electron transfer (ET) across a solid/electrolyte solution interface is broadly more complicated as compared with homogeneous redox processes. The first reason is the adsorption of reactant (product) for inner-sphere reactions, while the second complication results from a manifold of electronic energy levels which might contribute to the elementary act. The latter presumes a family of crossing free energy surfaces along the reaction coordinate which should be addressed when considering a heterogeneous charge transfer in terms of the quantum mechanical theories (see, for example, Refs. [1–4]). This issue is important for calculations of electronic transmission coefficient and can be treated analytically in two kinetic regimes: diabatic (i.e. weak electronic coupling) and adiabatic (strong coupling) limits. However, in the important intermediate region only numerical approaches seem to be efficient. Monte Carlo (MC) simulations which mimic a random walk through nodes of a 2D-lattice formed by crossing reaction free energy surfaces (RFES) along the solvent coordinate were performed first in work [5]; the crossing plots of RFES were considered in a linear approximation. Later this model was extended to parabolic RFES in Ref. [6]; the electrode overpotential effect was also partially addressed.

The aim of the present work is to elucidate three issues of heterogeneous ET using the MC technique employed in Ref. [5]. First of all we investigate not only normal but also activationless region when calculating an effective electronic transmission coefficient (κ). It has been shown in Refs. [7, 8] on the basis of quantum mechanical theory that for example, the reduction of the $[Fe(CN)_6]^{3-}$ and peroxodisulphate anions at a mercury electrode (thoroughly investigated experimentally by the Frumkin's school) proceeds in a near-activationsless region. Secondly, we consider in a more detail the dependence of κ on the electronic density of states (DOS) in an arbitrary region of orbital overlap. Finally the dependences of κ on the DOS and temperature for a bridge assisted ET are calculated as well. These problems were not discussed earlier in works [5, 6].

2. MODEL AND COMPUTATIONAL DETAILS

Let us consider for the sake of simplicity an outer-sphere one electron reduction proceeding at a metal electrode/electrolyte solution interface without bond break and with a small intramolecular reorganization. It is also assumed that the influence of the reactant—electrode orbital overlap on the activation barrier is small and can be neglected. Then the reaction energy

[1] This article is a contribution of the authors to the special journal issue dedicated to the centenary of the birth of outstanding electrochemist, corresponding member of the Academy of Sciences of the USSR, Veniamin Grigor'evich Levich (1917–1987).

[2] The article was translated by the authors.

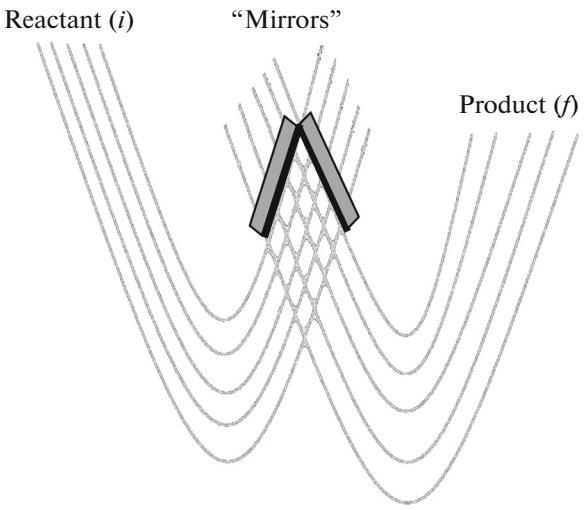

Fig. 1. Two-dimensional lattice formed by several crossing parabolic free energy surfaces along the reaction coordinate q.

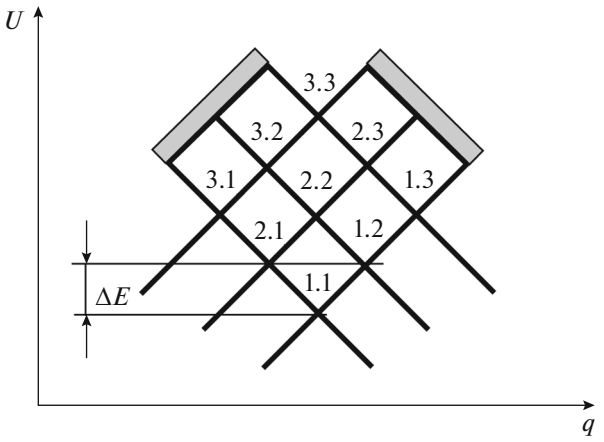

Fig. 2. Lattice nodes formed by three crossing reaction free energy surfaces; see also matrices (3) and (4).

surfaces describing the initial (reactant, i) and final (product, f) states are written as follows [4, 9],

$$U_i(q) = \lambda q^2 + m\Delta\varepsilon, \quad (1)$$

$$U_f(q) = \lambda(q-1)^2 + \Delta F + m\Delta\varepsilon, \quad (2)$$

where q is the dimensionless solvent coordinate, λ is the solvent reorganization energy, ΔF is the reaction free energy ($\Delta F = -e_0\eta$ and η is the electrode overpotential), $\Delta\varepsilon$ is the energy increment arising from a continuum of electronic states in the electrode and $m = 0, \pm1, \pm2,...$ ($m = 0$ corresponds to the Fermi level, negative and positive m values describe the electronic states below and above the Fermi level).

Equations 1, 2 presume that the Marcus theory [10] is employed to calculate the ET barrier. A family of crossing RFES is shown in Fig. 1. The coordinates of the lattice nodes can be readily calculated analytically using Eqs. (1)–(2). We present below for illustration a partial case, when the lattice is obtained by crossing of three $U_i(q)$ with three $U_f(q)$ energy surfaces (Fig. 2). A (3 × 3) matrix of the energy values looks as follows:

$$\begin{pmatrix} \frac{(\lambda+\Delta F)^2}{4\lambda} - \Delta\varepsilon & \frac{(\lambda+\Delta F+\Delta\varepsilon)^2}{4\lambda} - \Delta\varepsilon & \frac{(\lambda+\Delta F+2\Delta\varepsilon)^2}{4\lambda} - \Delta\varepsilon \\ \frac{(\lambda+\Delta F-\Delta\varepsilon)^2}{4\lambda} & \frac{(\lambda+\Delta F)^2}{4\lambda} & \frac{(\lambda+\Delta F+\Delta\varepsilon)^2}{4\lambda} \\ \frac{(\lambda+\Delta F-2\Delta\varepsilon)^2}{4\lambda} + \Delta\varepsilon & \frac{(\lambda+\Delta F-\Delta\varepsilon)^2}{4\lambda} + \Delta\varepsilon & \frac{(\lambda+\Delta F)^2}{4\lambda} + \Delta\varepsilon \end{pmatrix}. \quad (3)$$

In turn, the corresponding matrix of the solvent coordinates takes the form:

$$\begin{pmatrix} \frac{\lambda+\Delta F}{\lambda} & \frac{\lambda+\Delta F+\Delta\varepsilon}{\lambda} & \frac{\lambda+\Delta F+2\Delta\varepsilon}{\lambda} \\ \frac{\lambda+\Delta F-\Delta\varepsilon}{\lambda} & \frac{\lambda+\Delta F}{\lambda} & \frac{\lambda+\Delta F+\Delta\varepsilon}{\lambda} \\ \frac{\lambda+\Delta F-2\Delta\varepsilon}{\lambda} & \frac{\lambda+\Delta F-\Delta\varepsilon}{\lambda} & \frac{\lambda+\Delta F}{\lambda} \end{pmatrix}. \quad (4)$$

It follows from the Landau–Zener (LZ) theory [2–4] that the reaction system in the vicinity at each node can pass from the surface $U_i(q)$ on $U_f(q)$ (or in vice versa, from $U_f(q)$ on $U_i(q)$) with some probability (see Fig. 3). These probabilities are calculated as follows:

$$\vec{P}_i = (1 - \exp(-2\pi\gamma_e))f(\varepsilon)P_e, \quad (5)$$

$$\bar{P}_i = (1 - \exp(-2\pi\gamma_e))f(\varepsilon), \quad (6)$$

$$\vec{P}_f = (1 - \exp(-2\pi\gamma_e))(1 - f(\varepsilon)), \quad (7)$$

$$\bar{P}_f = (1 - \exp(-2\pi\gamma_e))(1 - f(\varepsilon))P_e, \quad (8)$$

where $2\pi\gamma_e$ is the Landay–Zener (LZ) factor, $f(\varepsilon)$ is the Fermi–Dirac distribution function and P_e is given by the Boltzmann factor, $\exp(-\Delta E/k_BT)$ (the meaning of ΔE is clear from Fig. 2).

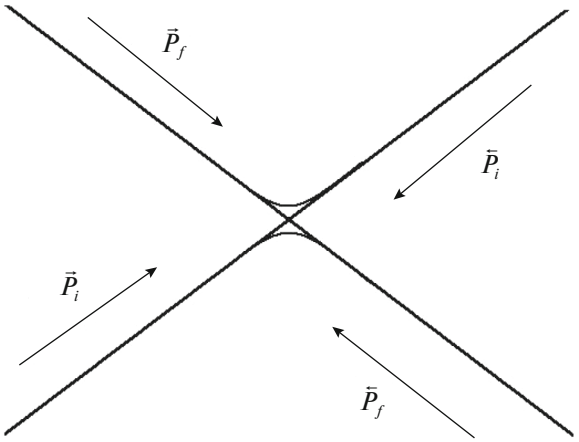

Fig. 3. Probabilities of transition from one reaction energy surface to another near their crossing point.

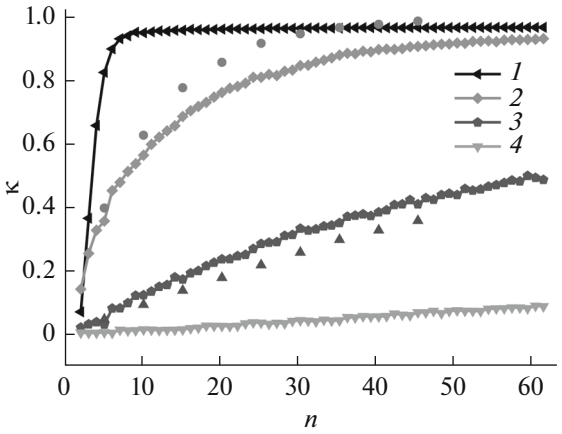

Fig. 4. Dependence of on the number of RFES (in a fixed energy interval) calculated for four different LZ factors: 0.99 (*1*), 0.1 (*2*), 0.01 (*3*), 0.001 (*4*) at η = 0 V and T = 298 K. The results of calculations in terms of the "multi-state" LZ theory (see Eq. (12)) are plotted as well: $2\pi\gamma_e$ = 0.1 (●), $2\pi\gamma_e$ = 0.01 (▲).

In Eqs. (5)–(8) $\vec{P}_i$ is the probability to pass on the lower right side of $U_f(q)$, $\bar{\vec{P}}_i$ is the probability to pass on the upper left side of $U_f(q)$, $\bar{\vec{P}}_f$ is the probability to pass on the lower left side of $U_f(q)$ and $\vec{P}_f$ is the probability to pass on the right upper side of $U_f(q)$.

Using our model we start the simulation loop from the lowest node in the left side of a rhombus formed by the crossing points (Figs. 1, 2). Then combining the Monte Carlo scheme with probability $\vec{P}_i$ one can arrange a random ballistic walk on the lattice nodes (see technical details in Ref. [5]). Instead of periodical boundary conditions we use the "mirror" closure, i.e. when the system attains the upper lattice sides (right and left), a new loop starts from the corresponding node ("reflection"). The efficiency of such an approach has been demonstrated earlier in work [5]. The trace formed by a number of the lattice nodes passed during such a rambling can be rendered as a trajectory. If trajectories start from some left lower node and finally reach the right lower lattice side, they are considered as successful. In contrast, if trajectories after some rambling return to the initial lattice side, they are called unsuccessful. The effective partial transmission coefficient (κ_i) can be defined as a ratio of the number of successful trajectories (N_{succes}) to the total number of attempts (N_{total}) to start from the selected node in the left lower lattice side:

$$\kappa_i = N_{\text{succes}} / N_{\text{total}}. \qquad (9)$$

A value of 300 for N_{total} was found to be enough for estimates with a reasonable accuracy. The same procedure is repeated for each node of the lower left side of rhombic lattice. Then the effective electronic transmission coefficient (κ) is calculated as follows:

$$\kappa = \frac{\sum_{i=1}^{n} \kappa_i \exp(-\Delta\varepsilon_i^* / k_B T)}{\sum_{i=1}^{n} \exp(-\Delta\varepsilon_i^* / k_B T)}, \qquad (10)$$

where n is the number of RFES left (or right), $\Delta\varepsilon_i^*$ is the energy difference between the i-th node and the lowest node.

Note that our definition of κ somewhat differs from that given in Ref. [6]. A value of 0.7 eV was taken for λ in Eqs. (1), (2) which nearly corresponds to the total reorganization energy of electron transfer at the electrochemical reduction of $[Fe(CN)_6]^{3-}$ [7]. A lattice 61 × 61 (i.e., n = 61) was used in most of simulations; in this case the difference between the bottom of the lowest und topmost RFES amounts to $7k_BT$. All MC simulations were performed by an original code written with the help of Matlab program package.

3. RESULTS AND DISCUSSION

In our simulations direct trajectories appear successful (see Eq. (9)), while unsuccessful trajectories are basically reverse (some examples are shown in Fig. A1, see Appendix A). The dependence of partial electronic transmission coefficient on the energy calculated from the Fermi level (ε_F) is plotted in Fig. A2 (Appendix A); a sharp decay of the curve in the region upper ε_F results from the Fermi–Dirac distribution. We have investigated first the dependence of κ on electronic density of states (DOS). The latter was modeled by a number of reaction free energy surfaces (n) in the abovementioned energy interval $7k_BT$. At

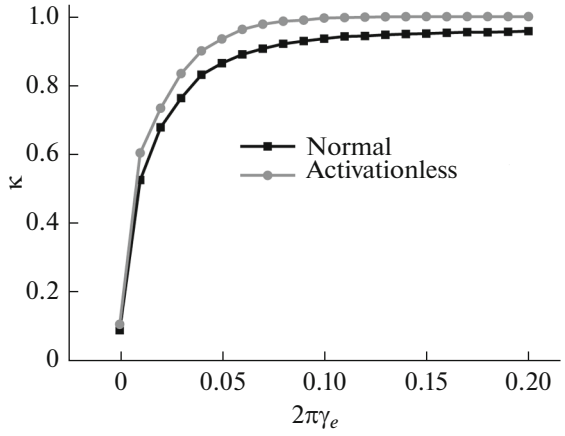

Fig. 5. Dependence of κ on the LZ factor calculated for the normal (η = 0) and activationless (η = 2.5 V) regions at T = 298 K.

small LZ factor values (0.01 and 0.001) our results predict nearly linear dependencies which are in a good qualitative agreement with the theory [1–4][3] (Fig. 4). For adiabatic limit the behaviour of transmission coefficient resembles a step-like function. In this limiting case κ practically does not depend on the DOS (i.e. on the electrode material) that looks reasonable and agrees with experiment [11]. Note that the transient interval at low DOS (where κchanges rapidly) seems to be artificial induced most likely by the discrete character of electronic energy level in the model system. On the other hand, a real dependence with the rapid change of electronic transmission coefficient might be observed for metal nanoclusters of different size with discrete energy spectrum.

The most challenging is, however an intermediate case ($2\pi\gamma_e = 0.1$), where κ reveals a significantly non-linear behaviour. Recently Feldberg and Sutin [12] treated the heterogeneous electron transfer in the whole range of orbital overlap (from diabatic to adiabatic limit) in the framework of "multistate" LZ theory:

$$\kappa = 1 - \exp[-2\pi\gamma_e\rho(\varepsilon_F)k_BT]. \quad (11)$$

We attempted to calculate similar dependencies at two different LZ factor values (0.01 and 0.1) and compare them with the results of MC simulations. It is convenient to recast Eq. (11) as follows,

$$\kappa = 1 - \exp[-2\pi\gamma_e\rho(\varepsilon_F)k_BT] = 1 - \exp[-2\pi\gamma_e n]. \quad (12)$$

On can see from Fig. 4 that using Eq. (12) overestimates the κ values for $2\pi\gamma_e = 0.1$ (with the maximal error 11%) and underestimate them for $2\pi\gamma_e = 0.01$ (with the maximal error 7%).

[3] According to Refs. [1–4] in diabatic limit $\kappa \approx 2\pi\gamma_e\rho(\varepsilon_F)k_BT$, where $\rho(\varepsilon_F)$ is the density of electronic states of an electrode in the vicinity of the Fermi level.

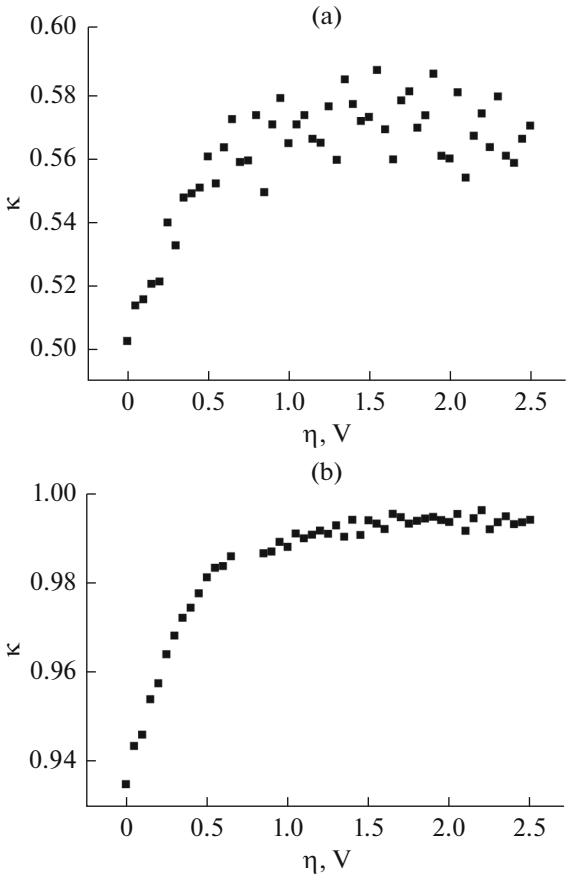

Fig. 6. Dependence of κ the electrode overpotential calculated at T = 298 K and two different values of the LZ factor: 0.01 (a) and 0.1 (b).

Electronic transmission coefficient as a function of the LZ factor is presented in Fig. 5 for two different kinetic regimes. The finite DOS (n = 61) was addressed in our simulations, that is why the calculated dependencies are strongly non-linear in the interval of $2\pi\gamma_e$ under consideration. As can be seen, the κ values for the activationless discharge exceed those obtained for the normal region but the maximal difference was found to be small and amounts to 0.08.

The electronic transmission coefficients calculated for two different LZ factors at n = 61 in a wide range of the electrode overpotentials are plotted in Fig. 6. The scattering of data for $2\pi\gamma_e = 0.01$ is explained by the fact that for the case of weak orbital overlap one needs longer simulations to collect results with a smaller dispersion. The qualitative effect was found to be the same for the both LZ factor values: κ increases with increasing η (ca by 0.06–0.08). It should be noted that the authors [6] have been reported a slight decreasing of the effective transmission coefficient with the overpotential growth. Again, this quantity was defined in work [6] in somewhat different way. The effects we observe originate purely from the rambling of reaction

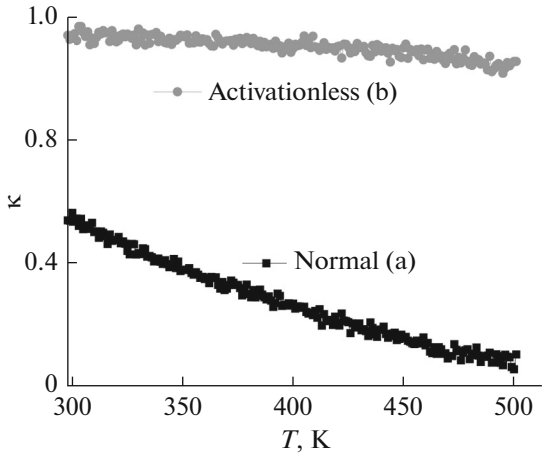

Fig. 7. Dependence of κ on temperature calculated for the normal (η = 0) and activationless (η = 2.5 V) regions at $2\pi\gamma_e = 0.1$.

system in the two-dimensional network (Fig. 1). On the other hand, the LZ factor depends on the tunneling matrix element (resonance integral) [1–4]. The latter is sensitive to the electronic density of a metal electrode and can noticeably increase at the growth of electrode overpotential. This significantly affects both the transmission coefficient [13] for diabatic ET reactions and the activation barrier of redox-processes in adiabatic limit [14].

The influence of temperature on effective transmission coefficient in the region of strong orbital overlap was explored as well. As demonstrated in Fig. 7a, at zero overpotential the κ values slightly decrease with increasing temperature. In general this effect should be even stronger, if the temperature dependence of LZ factor is additionally addressed[4]. However, for the activationless region the temperature effect is practically absent (Fig. 7b).

Finally some preliminary results obtained for a bridge assisted ET [4] are also reported. In this special case two LZ factors should be used in MC simulations: $2\pi\gamma_e^{(ib)}$ which describes ET from initial state to the bridge center and $2\pi\gamma_e^{(bf)}$ corresponding to ET from the intermediate to the final state. The corresponding simulation lattice is more complicated as compared with that in Fig. 1 because we need to consider an additional set of parabolic free energy surfaces describing a bridge molecule[5]. In further calculations we assume that $2\pi\gamma_e^{(ib)} = 0.01$ and $2\pi\gamma_e^{(bf)} = 0.99$. Qualitatively such a choice of the LZ factors agrees with the molecular model of Scanning Tunneling Microscope employed in work [15]. We omit other computational details which will be reported separately.

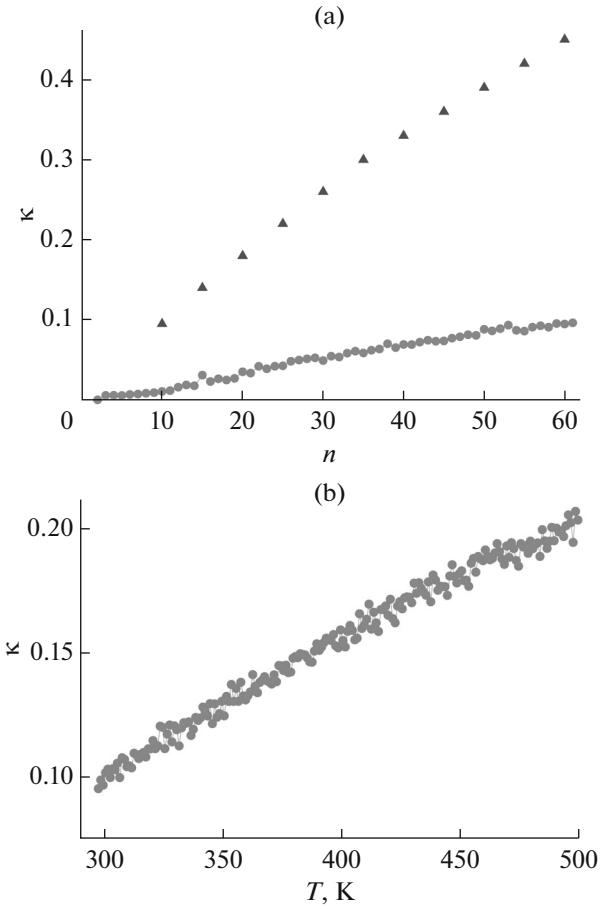

Fig. 8. Dependence of effective transmission coefficient in the bridge-assisted ET on the number of RFES (electronic density of states) (a) (▲—the results of calculations in terms of the "multistate" LZ theory, see Eq. (12)) and on temperature (b) calculated at η = 0.

The results differ from those discussed previously (Figs. 4, 7). The dependence of κon the DOS (Fig. 8a) was found to be significantly smaller in comparison with the direct electron transfer path ($2\pi\gamma_e = 0.01$). It is interesting to note that in this case the "multistate" LZ theory (Eq. (12)) strongly overestimate the effective transmission coefficient. The temperature effect (Fig. 8b) looks also more pronounced and even qualitatively different from that shown in Fig. 7.

4. CONCLUDING REMARKS

The heart of the model we employed in this work to describe heterogeneous ET reactions is a random ballistic walk on the two-dimensional network formed by crossing points of the reaction free energy surfaces. The model rests on the Monte Carlo technique and

[4] $\gamma_e \approx \sqrt{\pi/\lambda k_B T}$, see Refs.[3, 4].

[5] $U_b(q) = \lambda(q - 1/2)^2 + h + m\Delta\varepsilon$, h is the energy separation between the $U_b(q)$ minimum and the crossing point of $U_i(q)$ and $U_f(q)$ (see Eqs. (1), (2)). A value of 0.5 eV was used in our simulations, which presumes the "super-exchange" mechanism of electron transfer via a bridge molecule.

was proven to be robust and flexible to address different kinetic regimes. Emphasis was put on investigations of the influence of the electrode overpotential, DOS and temperature on the effective electronic transmission coefficient. The effects we observed are broadly interesting from a qualitative viewpoint albeit quantitatively they are rather small. Some preliminary results obtained for the bridge assisted ET look promising and call for a more detailed investigation. It has been also shown that the "multistate" LZ model [13] broadly does not provide reliable results in the intermediate interval of electronic coupling. It is evident that most of our findings are very difficult to check directly in electrochemical experiment. We believe, therefore that MC simulations in the framework of a two-dimensional lattice model are a useful tool and make it possible to gain a deeper insight into some details of the mechanism of heterogeneous electron transfer in a wide region of orbital overlap.

A while ago Schmickler and Mohr made an interesting attempt to describe the electron transfer across electrochemical interfaces in the whole range of electrode—reactant interactions (including both diabatic and adiabatic limits) [16, 17]. The authors addressed neither Landau–Zener theory, nor a manifold of the RFES and therefore did not deal with electronic transmission coefficient. Instead of this they have employed the Anderson–Newns formalism and found non-perturbative analytical expressions for the time-dependent occupation number of reactant, as well as for the rate constant which looks in diabatic limit similar to that found earlier in terms of the perturbation theory [1–4]. In work [17] the rate constant of electron transfer was calculated on the basis of simulations using the Brownian molecular dynamics, i.e., the solvent friction effects were considered as well. However, neither temperature, nor electrode overpotential effects on the rate constant were investigated. Ref. [18] should be also mentioned where the author combined the LZ theory with the Kramers approach to describe simple homogeneous redox processes. It would be tempting to combine in future our approach with the models developed in works [16, 17].

APPENDIX A

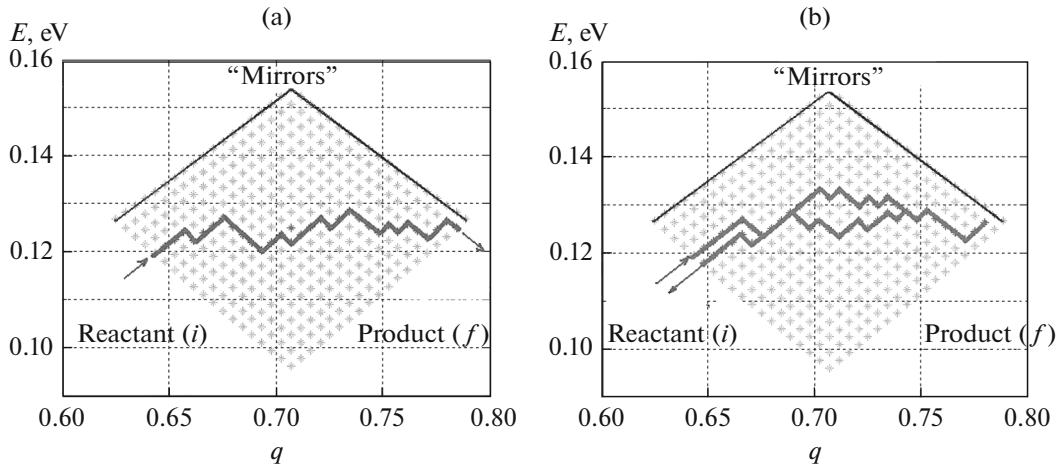

Fig. A1. Examples of "successful" (a) and "unsuccessful" (b) trajectories in MC simulations.

APPENDIX B

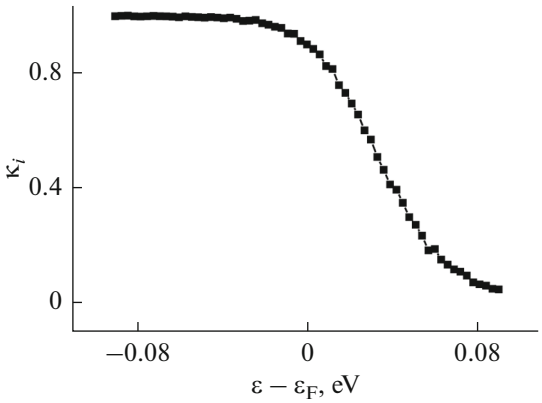

Fig. A2. Partial transmission coefficients as a function of the $\varepsilon - \varepsilon_F$ difference ($\eta = 1$ V, $2\pi\gamma_e = 0.1$, $T = 300$ K).

ACKNOWLEDGMENT

We thank Prof. Marshall Newton for stimulating interest to some aspects of our model and Dr. Tamara Zinkicheva for technical assistance. This work was partially supported by the RFBR (project no. 17-03-00619a).

REFERENCES

1. Levich, V.G., *Kinetics of Reactions with Charge Transfer, in Physical Chemistry, an Advanced Treatise*, Eyring, H., Henderson, D., and Jost, W., Eds., N.Y.: Acad. Press, 1970, vol. Xb.
2. Dogonadze, R.R. and Kuznetsov, A.M., *Progress in Surface Science*, 1975, vol. 6, pp. 1–41.
3. Kuznetsov, A.M., *Charge Transfer in Physics, Chemistry and Biology. Mechanisms of Elementary Processes and Introduction to the Theory*, Berkshire: Gordon and Breach Science Publishers, 1995.
4. Kuznetsov, A.M. and Ulstrup, J., *Electron Transfer in Chemistry and Biology*, Chichester, UK: Wiley, 1999.
5. Kuznetsov, A.M., Nazmutdinov, R.R., and Schmickler, W., Monte Carlo simulations of the electrochemical electron transfer processes, *J. Electroanal. Chem.*, 2002, vol. 532, pp. 171–180.
6. Kokkanen, A.A., Kuznetsov, A.M., and Medvedev I.G., Approximate method for calculation of electron transition probability for simple outer-sphere electrochemical reactions, *Russ. J. Electrochem.*, 2008, vol. 44, pp. 397–407.
7. Nazmutdinov, R.R., Glukhov, D.V., Tsirlina, G.A., and Petrii, O.A., Activationless reduction of a hexacyanoferrate anion at a mercury electrode, *Russ. J. Electrochem.*, 2003, vol. 39, pp. 97–107.
8. Nazmutdinov, R.R., Glukhov, D.V., Tsirlina, G.A., and Petrii, O.A., Molecular description of the persulphate ion reduction on a mercury electrode, *Russ. J. Electrochem.*, 2002, vol. 38, pp. 720–731.
9. Nazmutdinov, R.R., Bronshtein, M.D., Zinkicheva, T.T., and Glukhov, D.V., Modeling of electron transfer across electrochemical interfaces: State-of-the art and challenges for quantum and computational chemistry, *Int. J. Quantum Chem.*, 2016, vol. 116, pp. 189–201.
10. Marcus, R.A., On the theory of oxidation-reduction reactions involving electron transfer. I., *J. Chem. Phys.*, 1956, vol. 24, pp. 966–978.
11. Iwasita, T.I., Schmickler, W., and Schultze, J.W., Influence of the metal on the kinetics of outer sphere redox reactions, *Berichte der Bunsenges. Phys. Chem. Chem. Phys.*, 1985, vol. 89, pp. 138–142.
12. Feldberg, S.W. and Sutin, N., Distance dependence of heterogeneous electron transfer through the nonadiabatic and adiabatic regimes, *Chem. Phys.*, 2006, vol. 324, pp. 216–225.
13. Kornyshev, A.A., Kuznetsov, A.M., and Ulstrup, J., Effect of overpotential on the electronic tunnel factor in diabatic electrochemical processes, *J. Phys. Chem.*, 1994, vol. 98, pp. 3832–3837.
14. Nazmutdinov, R.R., Schmickler, W., and Kuznetsov, A.M., Microscopic modeling of the reduction of a Zn(II) aqua-complex on metal electrodes, *Chem. Phys.*, 2005, vol. 109, pp. 257–268.
15. Zhang, J., Chi, Q., Nazmutdinov, R.R., Zinkicheva, T.T., and Bronshtein, M.D., Submolecular electronic mapping of single cysteine molecules by in situ scanning tunneling imaging, *Langmuir,* 2009, vol. 25, pp. 2232–2240.
16. Mohr, J. and Schmickler, W., Exactly solvable quantum model for electrochemical electron transfer reactions, *Phys. Rev. Lett.*, 2000, vol. 85, pp. 1051–1054.
17. Schmickler, W. and Mohr, J., The rate of electrochemical electron transfer reactions, *J. Chem. Phys.*, 2002, vol. 117, pp. 2867–2872.
18. Schmickler, W., The rate of electron transfer reactions in the diffusive limit, *Cond. Matt. Phys.*, 2001, vol. 4, pp. 773–778.